

Simulating a White Dwarf-dominated Galactic Halo

Chris B. Brook, Daisuke Kawata & Brad K. Gibson

Centre for Astrophysics & Supercomputing, Swinburne University, Mail #31, P.O. Box 218, Hawthorn, Victoria, 3122, Australia

ABSTRACT

Observational evidence has suggested the possibility of a Galactic halo which is dominated by white dwarfs (WDs). While debate continues concerning the interpretation of this evidence, it is clear that an initial mass function (IMF) biased heavily toward WD precursors ($1 < m/M_{\odot} < 8$), at least in the early Universe, would be necessary in generating such a halo. Within the framework of homogeneous, closed-box models of Galaxy formation, such biased IMFs lead to an unavoidable overproduction of carbon and nitrogen relative to oxygen (as measured against the abundance patterns in the oldest stars of the Milky Way). Using a three-dimensional Tree N-body smoothed particle hydrodynamics code, we study the dynamics and chemical evolution of a galaxy with different IMFs. Both invariant and metallicity-dependent IMFs are considered. Our variable IMF model invokes a WD-precursor-dominated IMF for metallicities less than 5% solar (primarily the Galactic halo), and the canonical Salpeter IMF otherwise (primarily the disk). Halo WD density distributions and C,N/O abundance patterns are presented. While Galactic haloes comprised of $\sim 5\%$ (by mass) of WDs are not supported by our simulations, mass fractions of $\sim 1\text{-}2\%$ cannot be ruled out. This conclusion is consistent with the present-day observational constraints.

Subject headings: galaxies: formation — galaxies: evolution — Galaxy: halo — dark matter

1. Introduction

Evidence gathered by microlensing surveys toward the Large Magellanic Cloud suggest that a substantial fraction of the Milky Way's dark matter halo is comprised of $\sim 0.5 M_{\odot}$ objects - the MACHO Team claim 20% of the halo's dynamical mass may be tied up in these half-solar mass constituents (Alcock et al. 2000), while the EROS Team favour an upper limit of 30% (Lasserre et al. 2000). Constraints set by Hubble Space Telescope red star counts (Flynn et al. 1996) rule out large numbers of low-mass hydrogen burning stars

in the halo. By process of elimination, white dwarfs (WDs) represent one potential baryonic candidate for these microlensing events. This would correspond to of order 2×10^{11} WDs out to a distance of 60 kpc in the Galactic halo (see Zitrisky 1999).

The apparent identification of 2-5 high-proper motion WDs in the Hubble Deep Field-North supported the WD-dominated halo hypothesis (Ibata et al. 1999), as did the colour analysis of the Hubble Deep Field-South (Mendez et al. 2000) - the Ibata et al. claim though has since been retracted (Richer 2001). Ground-based searches for nearby high-proper motion WDs initially suggested a WD halo mass fraction of 10% (Ibata et al. 2000), although Flynn et al. (2001) favoured $\sim 2\%$. Based upon dynamical arguments and Galactic winds driven by a putative population of WD progenitors, Zhao (2002) suggest a fraction $< 4\%$. Regardless, Oppenheimer et al. (2001, hereafter OHDHS) have recently revived the WD-dominated halo picture with their claim that $> 2\%$ of the halo is made up of WDs. While criticism of the OHDHS analysis abounds (Gibson & Flynn 2001; Reid et al. 2001; Koopmans & Blandford 2002; Reyl e et al. 2001; Flynn et al. 2002; Torres et al. 2002), their result¹ (if confirmed) may yet be made consistent with the MACHO and EROS Team² results.

WDs represent the end point in the life cycle of stars whose initial masses are in the approximate range $1 - 8 M_{\odot}$. Populating a WD-dominated Galactic halo, in conjunction with a standard stellar initial mass function (IMF), would lead to a corresponding increase in the production of Type II supernovae (SNeII) and the rapid overproduction of heavy elements (Gibson & Mould 1997, hereafter GM97). In addition, the expected number of low-mass red dwarfs would violate the deep halo star counts of Flynn et al. (1996). These high- and low-mass “constraints” imply that a standard IMF cannot be employed to populate a putative WD-dominated Galactic halo. Instead, the IMF would have had to have been comprised almost exclusively of stars in the range $1 < m/M_{\odot} < 8$ - such WD-heavy IMFs have been discussed in the literature by Chabrier et al. (1996 - hereafter C96) and Adams & Laughlin (1996).

Besides the requirement that any WD-heavy IMF be restricted to $1 < m/M_{\odot} < 8$, there is an additional constraint provided by the observed abundance patterns in Population II

¹In addition to that of Nelson et al. (2002), who claim a 7% WD dark halo based upon 24 candidate high-proper motion objects in the Groth Strip, and Mendez (2002), who claims (based upon one apparent high-proper motion white dwarf seen towards NGC 6397) that most of the dark matter in the solar vicinity can be accounted for by halo and thick-disk white dwarfs.

²The EROS-2 white dwarf proper motion survey find that the halo white dwarf fraction cannot exceed 5% (95% c.l.).

halo stars. GM97 found that a WD-dominated IMF (wdIMF) inevitably leads to the overproduction of carbon and nitrogen relative to oxygen - *by more than an order of magnitude* - in comparison with that seen in the oldest stars of the Milky Way's halo. This result is a natural consequence of the life cycle of low- and intermediate-mass stars, stars which are responsible for synthesising the majority of the carbon and nitrogen in the Universe. Fields et al. (2000) confirmed the analysis of GM97, concluding that the halo carbon and nitrogen argument provides the strictest constraint to any WD-dominated halo scenario.

While there is no compelling direct evidence for variable IMFs, *at the present time* (e.g. Gilmore 2001), several theoretical studies suggest that the IMF of the first generation of stars (so-called Population III) might be quite different from that of the canonical Salpeter IMF (sIMF). Direct simulation attempts to form Pop III stars indicate an IMF biased toward super massive stars ($M > 100 M_{\odot}$) rather than white dwarf progenitors (Abel, Bryan & Norman 1999, 2002). It is the lack of metals, which cause cloud fragmentation of gas in star forming regions, that results in such a top heavy IMF (see also Bromm et. al 2001). Other studies also indicate a different IMF for Pop III stars, e.g., Yoshii & Saio (1987) and Nakamura & Umemura (2001), which suggested a bimodal IMF making large numbers of super massive stars around $100 M_{\odot}$ and a futher peak in the intermediate, white dwarf progenitor mass range. It is possible that the stars from the high mass peak of such an IMF would not contribute to chemical enrichment due to the formation of black holes, thus making such an IMF effectively favour white dwarf progenitors. This Pop III IMF is expected to apply to the first generation of halo stars - the generation which would manifest itself *now* in the population of putative high-proper motion stellar halo WDs. Such studies remain, however, highly uncertain. Our motivation for invoking the wdIMF remains the MACHO observations and the necessity for invoking such an IMF in order for these observations to be explained by a large population of white dwarf stars populating the halo. In addition to the wdIMF and sIMF possibilities, in what follows we will also consider a variable IMF in which stars formed from the low (high) metallicity gas are distributed following the adoption of the wdIMF (sIMF). One can anticipate that while the wdIMF phase will invariably lead to high C/O and N/O ratios (as discussed by GM97), the subsequent sIMF phase can ameliorate this effect. This variable IMF scenario was not considered by GM97.

The currently favoured hierarchical clustering scenario of galaxy formation postulates that star formation progresses through the on-going accretion of galactic building blocks. Within this framework, highly inhomogeneous chemical evolution occurs; the assumption of homogeneous closed-box models for the Milky Way's evolution (as was admittedly adopted by GM97) are no longer suitable. The early phases of galaxy formation demand a chemodynamical approach, one which we adopt here explicitly within the context of the WD-dominated IMF hypothesis. In what follows, we examine the ability of metallicity-dependent

variable IMFs to resolve the apparent contradiction between a significantly WD-heavy Galactic halo and the C/O and N/O abundance patterns of halo stars. To achieve this, we perform numerical simulations which calculate self-consistently the chemical and dynamical evolution of a Milky Way-like galaxy.

In Section 2, we describe our numerical methods, concentrating upon the code itself and our treatments of star formation, IMFs, and energy feedback to the interstellar medium (ISM). Section 3 presents the results of our simulations in terms of resulting white dwarf halo densities, and Galactic chemical evolution of carbon, nitrogen, and oxygen. The implications for a WD-dominated Galactic dark matter halo are described in Section 4.

2. Method

2.1. The Code

Our simulations were performed using a modified version of the software package described by Kawata (1999, 2001). An overview of the code is provided here along with the relevant modifications made for the current study - the reader is referred to Kawata (1999, 2001) for all other details. Our code is based upon the Hernquist & Katz 1989 and Katz, Weinberg & Hernquist 1996 *TreeSPH*, combining a tree algorithm (Barnes & Hut 1986) with smoothed particle hydrodynamics (SPH) (Lucy 1977; Gingold & Monaghan 1977) for the computation of gravitational forces and numerical hydrodynamics respectively. This three-dimensional code is fully Lagrangian, with individual smoothing lengths and time steps making it highly adaptive in space and time. It includes a self-consistent treatment of physical processes governing galaxy formation, including self-gravity, hydrodynamics, radiative cooling, star formation, supernovae feedback, and metal enrichment. We employ metallicity-dependent gas cooling rates derived from MAPPINGS III (Sutherland & Dopita 1993); their implementation is described by Kawata & Gibson (2003).

2.1.1. Star Formation

Star formation prescriptions similar to those of Katz (1992) and Katz, Weinberg & Hernquist (1996) were employed. Star formation occurs whenever

1. the gas density is greater than a critical density:
 $\rho_{crit} = 2 \times 10^{-25} \text{ g cm}^{-3}$ (Katz et al. 1996), and

2. the gas velocity field is convergent: $\nabla \cdot v_i < 0$.

Our adopted star formation law is written

$$\frac{d\rho_*}{dt} = -\frac{d\rho_g}{dt} = \frac{c_*\rho_g}{\tau_g} \quad (1)$$

where $\frac{d\rho_*}{dt}$ is the star formation rate (SFR). Equation 1 corresponds to a Schmidt law in which the SFR is proportional to $\rho_g^{1.5}$. The dynamical timescale of the gas is given by $\tau_g = \sqrt{(3\pi/16G\rho_g)}$; in regions eligible for star formation, this dynamical timescale is generally longer than the cooling timescale. Star formation efficiency is parameterised by the dimensionless parameter c_* , which, after Kawata (1999, 2001), was set to $c_* = 0.5$.

Equation 1 implies that the probability, p_* , with which one gas particle entirely transforms into a star particle during a discrete time step, Δt , is $p_* = 1 - \exp(-c_*\Delta t/t_g)$. This avoids an intolerably large number of star particles of different masses being formed. The newly created star particle behaves as a collisionless particle.

2.1.2. Initial Mass Functions

In our *TreeSPH* simulations, “stars” are represented as particles with a typical mass of order $10^5 M_\odot$; the relative number distribution of stellar masses within a “particle” is governed by the assumed initial mass function (IMF). Fundamental to our modeling is the adoption of the Chabrier et al. (1996) white dwarf progenitor-dominated IMF (wdIMF). We represent this IMF by a truncated power-law of the form

$$\Phi(m) dm = dn/dm = Ae^{-(\bar{m}/m)^\beta} \times m^{-\alpha} dm \quad (2)$$

for which we use $\bar{m} = 2.7$, $\beta = 2.2$, and $\alpha = 5.75$. The peak of this wdIMF occurs at $m \approx 2 M_\odot$, favouring the production of WD progenitors.

The canonical Salpeter (1955) IMF (sIMF) is used to describe the local stellar mass function (by number) and is written

$$\Phi(m)dm = dn/dm = Am^{-(1+x)} dm, \quad (3)$$

with $x=1.35$. The sIMF (solid line) and wdIMF (dashed line) are shown in Figure 1.

The coefficient A in equations 2 and 3 is determined by normalising the respective IMFs over the mass range $0.1 \leq m/M_\odot \leq 40.0$. We will explore simulations in which the adopted IMF is invariant in space and time (and governed by either the wdIMF or sIMF functions),

as well as metallicity-dependent models (in which star formation in regions where the gas metallicity is less than 5% solar is governed by the wdIMF form, with the sIMF form applying otherwise).

We will compare the results of our simulations using these very different IMF assumptions in terms of their chemical evolution properties, and contrast their inherent inhomogeneous nature with the original homogeneous models of GM97. Each IMF assumption also leads to very different outcomes for the halo and disk WD densities, an issue we return to in Section 3.

2.1.3. Feedback

Type II supernovae (SNeII) are assumed to be the end result for all stars of mass $m \geq 10 M_{\odot}$. These massive stars explode within the simulation time step in which they are born, and so the instantaneous recycling approximation (for the nucleosynthetic products associated with these stars) applies. SNeII release thermal and mechanical energy to the surrounding interstellar medium, in addition to their stellar yields; we assume that each supernova releases 10^{50} erg of thermal energy. For SNeII, the metallicity-dependant stellar yields of Woosley & Weaver (1995) are adopted.

For low- and intermediate-mass stars, we use the stellar yields of van den Hoek & Groenewegen (1997). The lifetimes of these stars are significantly longer than the time steps of our simulations, and so the instantaneous recycling approximation is relaxed; we assume that recycling from intermediate mass stars occurs after a fixed time delay. Weighting by the IMF slope, over the range $1 \leq m/M_{\odot} \leq 8$, the typical mass is $\sim 2 M_{\odot}$ (for both the wdIMF and sIMF); we therefore adopt a delay of 1 Gyr, corresponding to the main sequence lifetime of a $2 M_{\odot}$ star (Schaller et al. 1992).

For the current study, we ignore the effects of Type Ia supernovae. As noted by GM97, these supernovae do not produce significant amounts of carbon, nitrogen, or oxygen (relative to SNeII), elements which form the basis of the analysis which follows.

The mass, energy and heavy elements are smoothed over the neighbouring gas particles using the SPH smoothing algorithm. For example, in the timestep in which mass is released from a star particle due to a Type II supernova explosion, the increment of the mass of the j -th neighbour particle is

$$\Delta M_{SN,j} = \frac{m_j}{\rho_{g,i}} M_{SN,i} W(r_{ij}, h_{ij}) \quad (4)$$

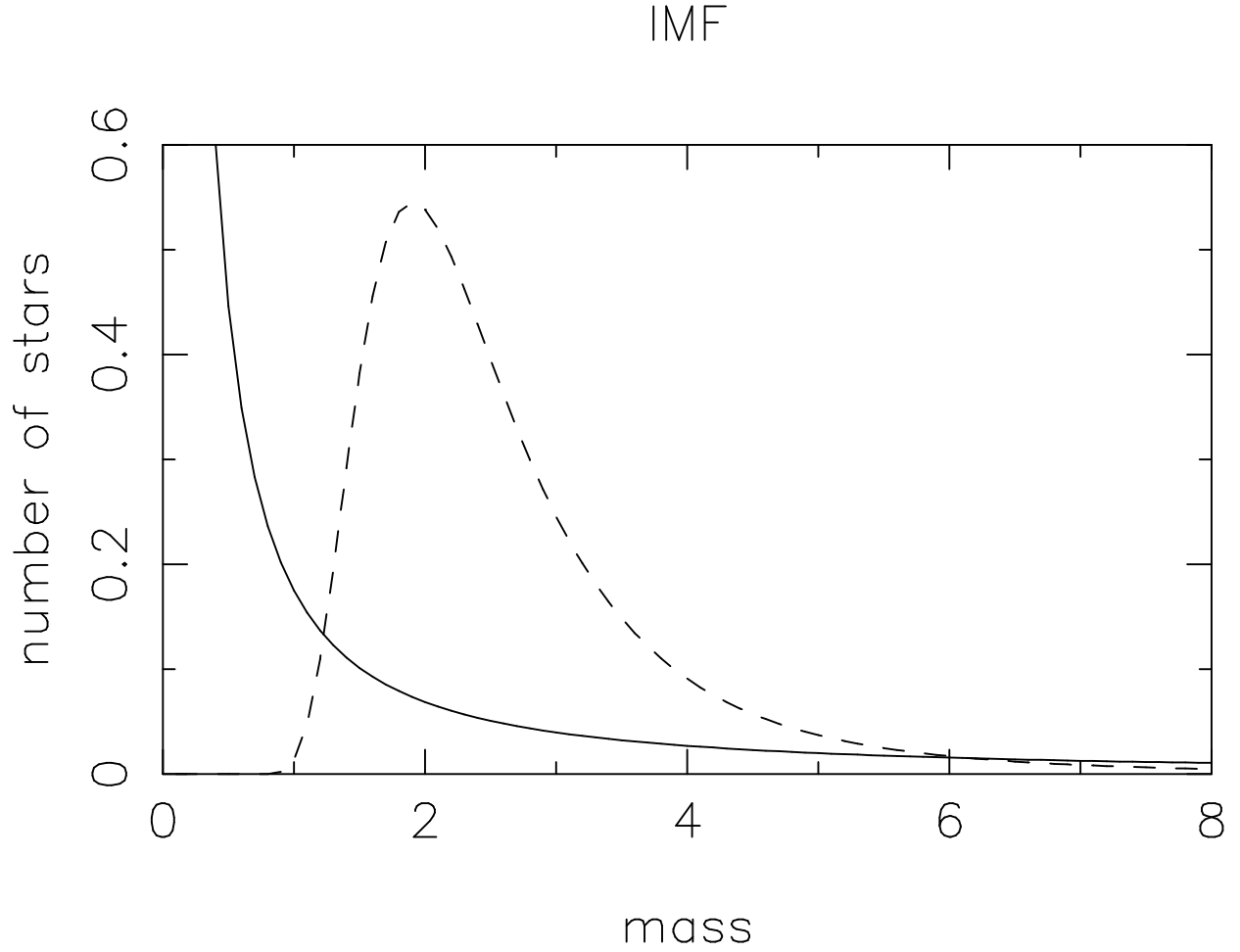


Fig. 1.— Comparison of the Salpeter (1955) (solid line) and Chabrier et al. (1996) (dashed line) IMFs; the latter is dominated by white dwarf progenitors. Both IMFs have been normalised to unity over the mass range $0.1 \leq m/M_{\odot} \leq 40.0$.

where

$$\rho_{g,i} = \langle \rho_g(x_i) \rangle = \sum_{j \neq i} m_j W(r_{ij}, h_{ij}) \quad (5)$$

and $W(r_{ij}, h_{ij})$ is an SPH kernel.

Tables 1 (SNeII) and 2 (low- and intermediate-mass stars) list the IMF-weighted stellar yields (in solar masses ejected per solar mass of stars formed) adopted in our analysis; in both tables, the first block represents the sIMF yields and the second block, the wdIMF. Four (three) different metallicities are highlighted for massive (intermediate mass) stars.

The overproduction of carbon and nitrogen with respect to oxygen, for IMFs dominated by white dwarf precursors, can be best appreciated by referral to Figure 2. Shown here are the adopted stellar yields’ $[C,N/O]^3$ as a function of initial mass; both $[C/O]$ and $[N/O]$ are significantly in excess of solar for $m \leq 8 M_\odot$. In comparison, the oldest stars of the Galactic halo show $[C/O] \simeq [N/O] \simeq -0.5$ (Timmes, Woosley & Weaver 1995). We can anticipate that an IMF in which a large number of these intermediate mass stars are present will result in an over-abundance of carbon and nitrogen compared to solar abundances.

The uncertainty in the stellar yields of zero metallicity stars was one of the few caveats which accompanied the earlier semi-analytical models of GM97 and Fields et al. (2000). As noted by Marigo et al. (2001) “the distinct evolutionary behaviour of these (zero metallicity) stars may also imply a very distinct nucleosynthesis and chemical pollution of the interstellar medium”; at issue here is the production of carbon and nitrogen in Population III stars. *If* it could be shown that neither element was synthesised or ejected into the ISM in the early Universe, a “loophole” could then exist which would allow a WD-dominated Galactic halo without violating the elemental abundance patterns in the halo today. The new stellar evolution models described by Abia et al. (2001) suggest that large quantitative differences do not exist between extant low-metallicity models (which do undergo thermal pulses and eject significant carbon and nitrogen) and Population III (at least for masses $4 \leq m/M_\odot \leq 7$; for masses $m \leq 4 M_\odot$, the Population III yields remain uncertain). Our models are qualitatively robust against the specific choice of yield compilation.

2.2. The Model

We calculate semi-cosmological models, following the technique described by Kawata (1999, 2001). Our seed Galaxy is an isolated sphere upon which small-scale density fluc-

³ $[C/O] \equiv \log(C/O) - \log(C/O)_\odot$

Table 1: IMF-weighted stellar yields adopted for massive ($m \geq 10 M_{\odot}$) stars.

Metallicity	Salpeter (1955) - sIMF			
	$0.0 \leq Z/Z_{\odot} < 10^{-4}$	$10^{-4} \leq Z/Z_{\odot} < 10^{-1}$	$10^{-1} \leq Z/Z_{\odot} < 1.0$	$1.0 \leq Z/Z_{\odot}$
Element				
C	6.12×10^{-4}	8.46×10^{-4}	8.39×10^{-4}	8.53×10^{-4}
O	2.74×10^{-3}	5.99×10^{-3}	6.55×10^{-3}	7.26×10^{-3}
N	3.25×10^{-5}	3.20×10^{-5}	6.09×10^{-5}	3.05×10^{-4}
Ne	2.08×10^{-4}	7.32×10^{-4}	5.47×10^{-4}	6.92×10^{-4}
Mg	1.42×10^{-4}	2.83×10^{-4}	3.17×10^{-4}	4.14×10^{-4}
Si	1.80×10^{-4}	5.88×10^{-4}	6.06×10^{-4}	7.60×10^{-4}
Fe	4.78×10^{-4}	4.76×10^{-4}	7.86×10^{-4}	7.05×10^{-4}
[C/O]	-0.16	-0.35	-0.40	-0.44
[N/O]	-0.98	-1.33	-1.09	-0.44
		Chabrier et al. (1996) - wdIMF		
C	3.62×10^{-6}	5.49×10^{-6}	6.06×10^{-6}	5.77×10^{-6}
O	7.71×10^{-6}	1.47×10^{-5}	1.76×10^{-5}	2.12×10^{-5}
N	1.20×10^{-6}	1.21×10^{-6}	1.47×10^{-6}	3.31×10^{-6}
Ne	8.66×10^{-7}	6.14×10^{-6}	1.61×10^{-6}	3.07×10^{-5}
Mg	5.63×10^{-7}	7.32×10^{-7}	8.30×10^{-7}	1.36×10^{-6}
Si	1.72×10^{-6}	3.62×10^{-6}	2.92×10^{-6}	4.04×10^{-6}
Fe	6.00×10^{-6}	3.94×10^{-6}	1.02×10^{-5}	6.41×10^{-6}
[C/O]	0.167	0.067	0.032	-0.070
[N/O]	0.14	-0.14	-0.13	0.13

Table 2: IMF-weighted stellar yields adopted for low- and intermediate-mass ($m \leq 8 M_{\odot}$) stars.

Metallicity	Salpeter (1955) - sIMF		
	$5 \times 10^{-3} \leq Z/Z_{\odot} < 10^{-1}$	$10^{-1} \leq Z/Z_{\odot} < 1.0$	$1.0 \leq Z/Z_{\odot}$
Element			
C	6.82×10^{-4}	7.26×10^{-4}	1.20×10^{-3}
O	1.27×10^{-5}	1.18×10^{-4}	1.11×10^{-3}
N	1.32×10^{-3}	1.37×10^{-3}	1.21×10^{-3}
Ne	1.06×10^{-5}	1.56×10^{-5}	2.36×10^{-5}
Mg	5.95×10^{-7}	1.19×10^{-5}	1.26×10^{-4}
Si	6.46×10^{-7}	1.29×10^{-5}	1.36×10^{-4}
Fe	1.07×10^{-6}	2.14×10^{-5}	2.26×10^{-4}
[C/O]	2.22	1.28	0.529
[N/O]	2.95	2.00	0.97
		Chabrier et al. (1996) - wdIMF	
C	3.96×10^{-3}	3.10×10^{-3}	3.96×10^{-3}
O	7.67×10^{-5}	4.54×10^{-4}	4.31×10^{-3}
N	2.42×10^{-3}	1.43×10^{-3}	1.74×10^{-3}
Ne	3.32×10^{-5}	5.70×10^{-5}	8.60×10^{-5}
Mg	9.81×10^{-7}	4.47×10^{-5}	4.70×10^{-4}
Si	1.07×10^{-6}	4.85×10^{-5}	5.11×10^{-4}
Fe	1.76×10^{-6}	8.05×10^{-5}	8.48×10^{-4}
[C/O]	2.21	1.32	0.46
[N/O]	2.44	1.43	0.54

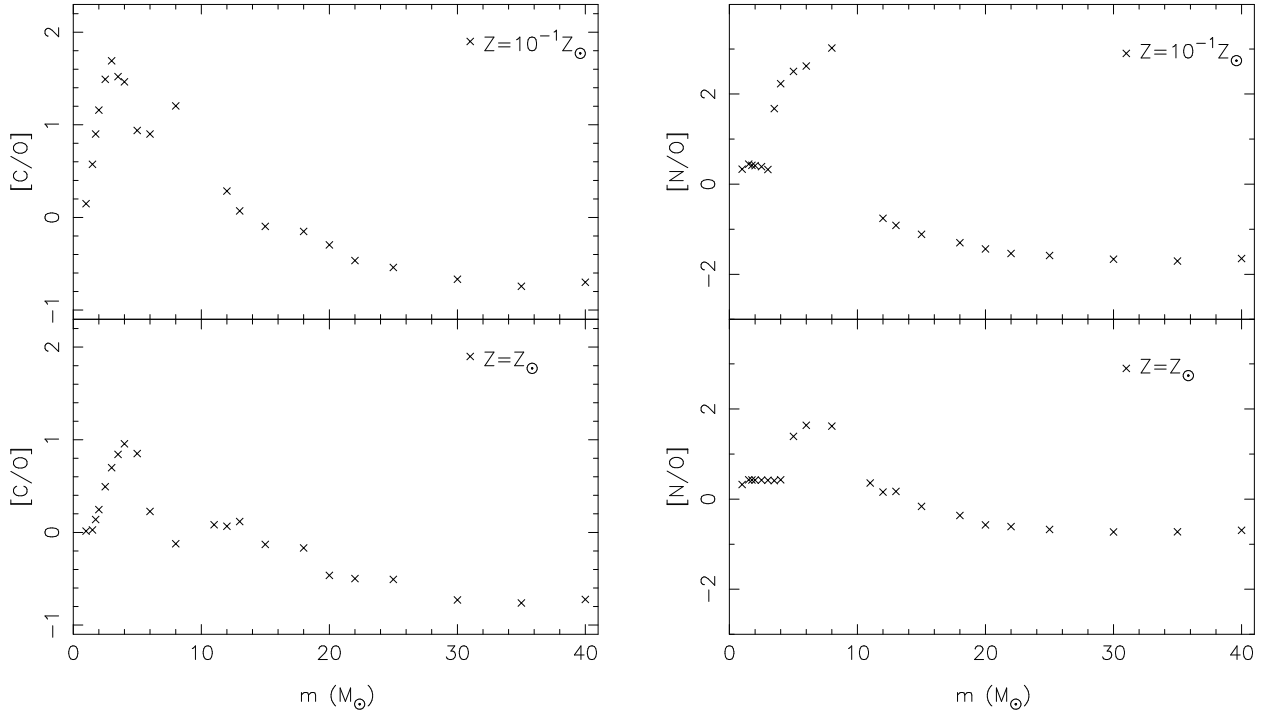


Fig. 2.— Ratio of carbon (left panels) and nitrogen (right panels) to oxygen for the adopted stellar yields - Woosley & Weaver (1995) yields were adopted for Type II supernova progenitors ($m \geq 10 M_{\odot}$), while the low- and intermediate-mass yields of van den Hoek & Groenewegen (1997) were used for $m \leq 8 M_{\odot}$.

tuations corresponding to a Cold Dark Matter (CDM) power spectrum are superimposed. These initial density fluctuations are generated using COSMICS (Bertschinger 1995). The effects of longer wavelength fluctuations are incorporated by enhanced density of the sphere and the application of a spin parameter λ responsible for initiating rigid rotation of the overdense sphere. This spin parameter is defined

$$\lambda \equiv \frac{J|E|^{1/2}}{GM_{tot}^{5/2}}, \quad (6)$$

where E is the total energy of the system, J the total angular momentum, M_{tot} the total mass of the sphere (dark matter + gas). Mass fluctuations (rms) in a sphere of radius $8h^{-1}$ Mpc are denoted $\sigma_{8,in}$, and normalise the amplitude of the CDM power spectrum. According to Katz & Gunn (1992) and Steinmetz & Muller (1995), a large value of $\sigma_{8,in}$ leads a large transfer of angular momentum from the gas particles to the dark matter particles, and a bulge larger than observed in the Milky Way; in order to avoid this, we consider the Galaxy to be formed in a an environment where the small scale density perturbation is smoother than the mean value suggested in standard CDM cosmology. We set $\sigma_{8,in} = 0.1$. The expected collapse redshift is given by z_c . The amplitude of the top-hat density perturbation δ_i is approximately related (Padmanabham 1993) to initial and collapse redshift by $z_c = 0.36\delta_i(1 + z_i) - 1$. Thus δ_i is determined for a given z_c at z_i . We set $z_c = 2.0$. The simulated galaxies described here have total mass $M_{tot} = 5 \times 10^{11} M_\odot$, approximating the total mass of the Milky Way within 50 kpc (Wilkinson & Evans 1999). For our models, the initial conditions are uniquely determined by the choice of λ , M_{tot} , $\sigma_{8,in}$, and z_c .

Using a comparable semi-cosmological model, Katz & Gunn (1991) found that a seed galaxy with a large spin parameter evolves into a disk system. Our best Milky Way models require $\lambda = 0.07$, in order to remain consistent with the Galaxy’s present-day disk properties. We assume a flat ($\Omega_o = 1$) universe with baryon fraction $\Omega_b = 0.1$ and Hubble constant $H_o = 50 \text{ km s}^{-1} \text{ Mpc}^{-1}$; evolution within isolated galaxy simulations using top hat overdensities are not greatly influenced by choice of cosmology. Evolution is traced from an initial redshift $z_i = 40$ to the present.

The initial conditions used are somewhat artificial, and will not exactly reflect hierarchical formation of the Milky Way as expected in CDM cosmologies. However, this approach still traces hierarchical build up of a galaxy, self consistently treating its chemical and dynamical history, and is sufficient for the purposes of documenting the effects between different IMFs.

Our study relies on the chemical enrichment processes of SPH, as described in section 2.1.3. In order to ensure that such processes are not determined by the resolution adopted, we perform the study at three different resolution regimes. The resolution regimes employ

6142, 18342, and 40958 particles (initially split evenly between gas and dark matter). The results presented in this paper are from the highest resolution models; the results of different resolution regimes varied only marginally quantitatively, and the analysis and conclusions presented hold in all three; we therefore only present the highest resolution models. Our highest resolution models have dark matter (baryonic) particles of mass $2.2 \times 10^6 M_\odot$ ($2.4 \times 10^5 M_\odot$), which is comparable in resolution with other recent simulations of disk galaxy formation (e.g. Abadi et. al 2003)⁴. The gravitational softening length is 0.79 kpc (1.6 kpc) for baryonic (dark matter) particles.

As noted earlier, the primary “variable” in our simulations is the initial mass function (IMF). Three different scenarios have been considered here - models 1 and 2 assume the Salpeter (1955) and Chabrier et al. (1996) IMFs, respectively, regardless of metallicity; model 3 assumes the Chabrier et al. IMF (wdIM) for metallicities below 5% solar, and the Salpeter IMF (sIMF) elsewhere, as summarised in Table 3.

3. Results

Figures 3 and 4 show the X-Y and X-Z projections of the morphological evolution for model 3, over the redshift range $z = 2.7$ to $z = 0.9$; models 1 and 2 are qualitatively similar. The Z-axis corresponds to the initial rotation axis. Sub-clumps associated with early star formation can be traced to initial small-scale density fluctuations, and are seen by redshift $z \approx 2.5$. These sub-clumps merge hierarchically until redshift $z \approx 1.7$; by redshift $z \approx 1.6$, large sub-clumps merging in the centre of the Galaxy (where the disk is forming) is responsible for the bulk of star formation. An epoch of accretion ($1.2 < z < 0.9$) sees a majority of the high-metallicity ($Z > 0.05 Z_\odot$) stars formed, and the disk-like structure of the Galaxy

⁴In galaxy formation simulations including cooling, the physical resolution determines the computational costs rather than the total number of particles.

Table 3: The three models adopted in the current analysis; the initial mass function (IMF) is the only variable.

Model	IMF	
	$Z < 0.05 Z_\odot$	$Z > 0.05 Z_\odot$
model 1	Salpeter	Salpeter
model 2	Chabrier	Chabrier
model 3	Chabrier	Salpeter

becomes evident. The star formation history of model 3 is shown in Figure 5. The system evolves little morphologically after redshift $z \approx 0.8$. While not shown, we confirm that the radial scale lengths for our simulated disk at $z = 0$ (both gas and stellar) match those of the Milky Way.

Density maps of the final distributions ($z = 0$) of star and gas particles for model 3 are shown in Figure 6. The X-Y (upper row) and X-Z (bottom row) planes are shown- the low-metallicity ($Z < 0.05Z_\odot$) stars of the Galaxy preferentially populate the halo and thick disk, while the metal-rich ($Z > 0.05Z_\odot$) component populates the bulge and thin disk.

3.1. White Dwarf dominated Halo

In this section we investigate whether our models 2 and 3 have resulted in a halo which contains a significant amount of mass tied up in white dwarf stars. We make a comparison of the resulting halo and disk white dwarf (WD) densities of our three models, derived using the different assumed IMFs. The halo stars are defined as star particles in the region $4 < R_{XYZ} < 20$ kpc and $|Z| > 4$ kpc. The *mean* halo white dwarf number densities n , for each of the IMF models discussed in § 2 are shown in Table 4, where n is defined as

$$n = \frac{1}{V} \sum_i m_{s,i} \int_{1M_\odot}^{8M_\odot} \Phi(m) dm \quad (7)$$

The summation is over star particles which are older than 1 Gyr (the lifetime of a $2 M_\odot$ stars, and also the time delay adopted in our chemical evolution modeling of white dwarf progenitors- recall Section 2.1.3) and found in the above region for the halo. It is important to note that the absolute values of the densities is sensitive to the definition of the region selected; the densities are shown to provide details of how the number densities of white dwarfs altered between the three models.

As expected, model 2 (Chabrier IMF at all metallicities) results in significantly more white dwarfs in the halo (by a factor of 3.8), when compared with model 1 (Salpeter IMF at all metallicities). The variable IMF of model 3 (Chabrier at low-metallicities and Salpeter elsewhere) results in a factor of 3.5 increase in the halo white dwarf population with respect to model 1. In other words, model 3 increases the number of halo white dwarfs to almost the same degree as model 2, when compared with the canonical Galactic models which use a Salpeter IMF alone (i.e., model 1). The ability of model 3 to increase the number of halo

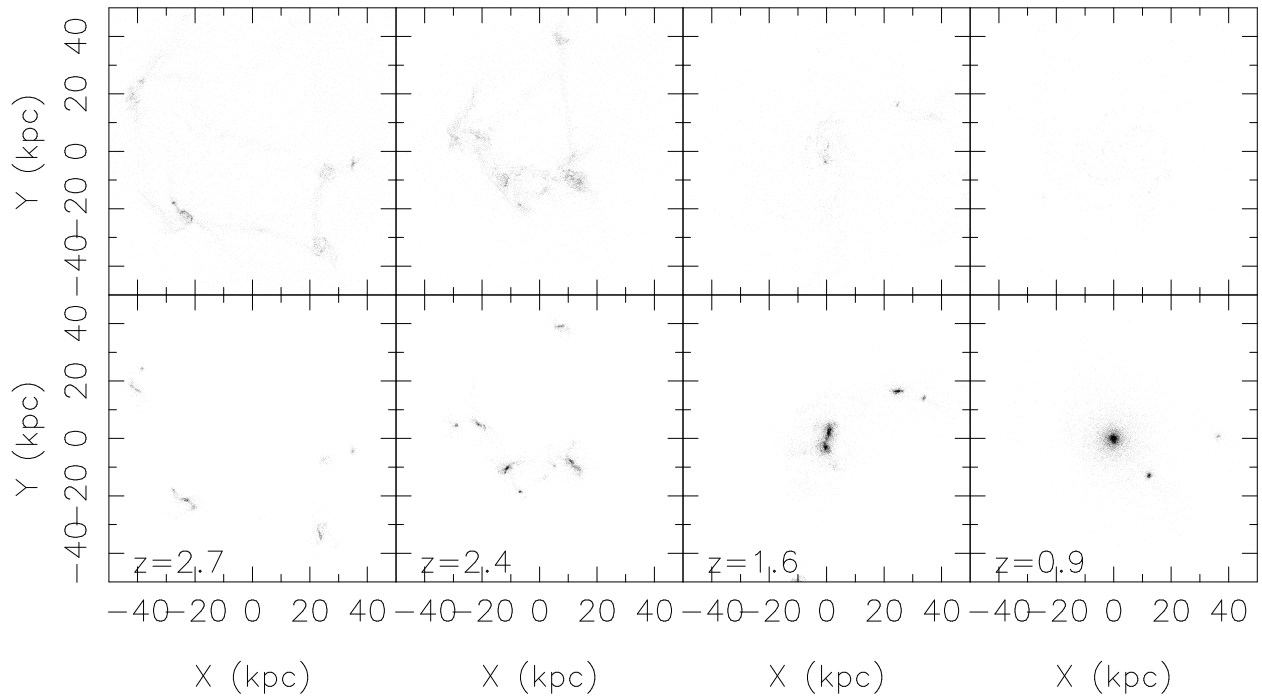


Fig. 3.— Projection onto the X-Y plane of the evolution of gas (upper row) and stars (bottom row) during the major star forming epoch of model 3.

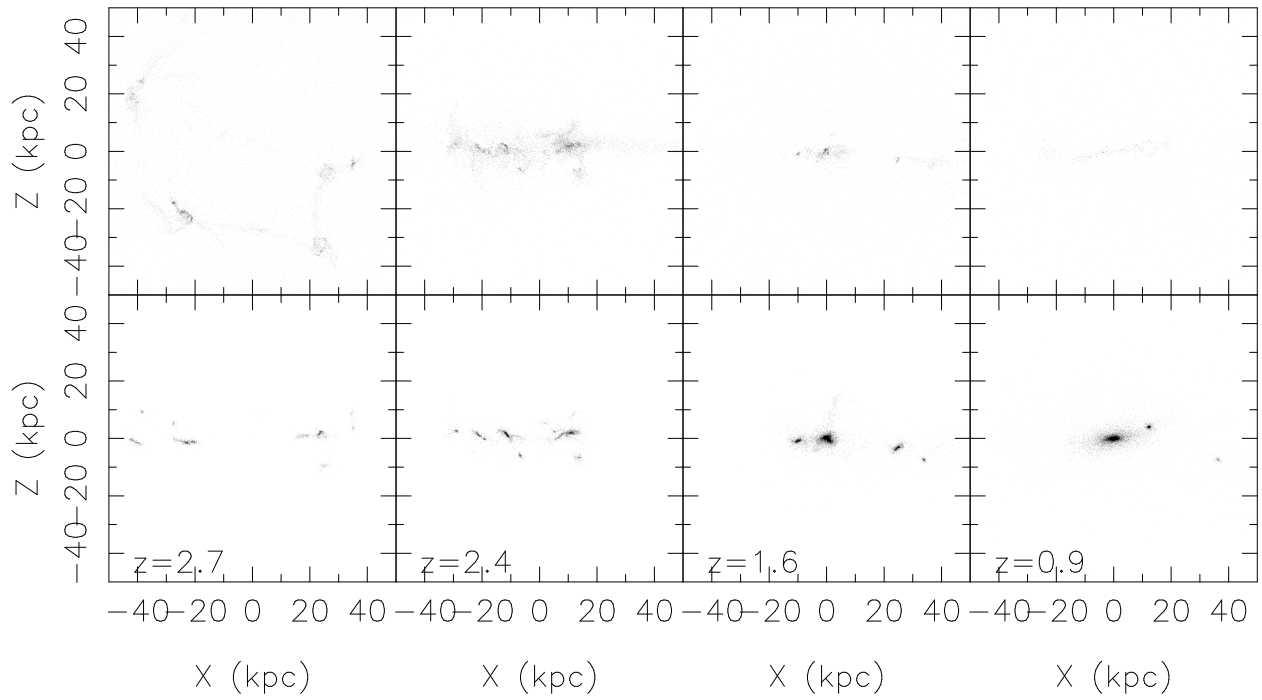


Fig. 4.— Projection onto the X-Z plane of the evolution of gas (upper row) and stars (bottom row) during the major star forming epoch of model 3.

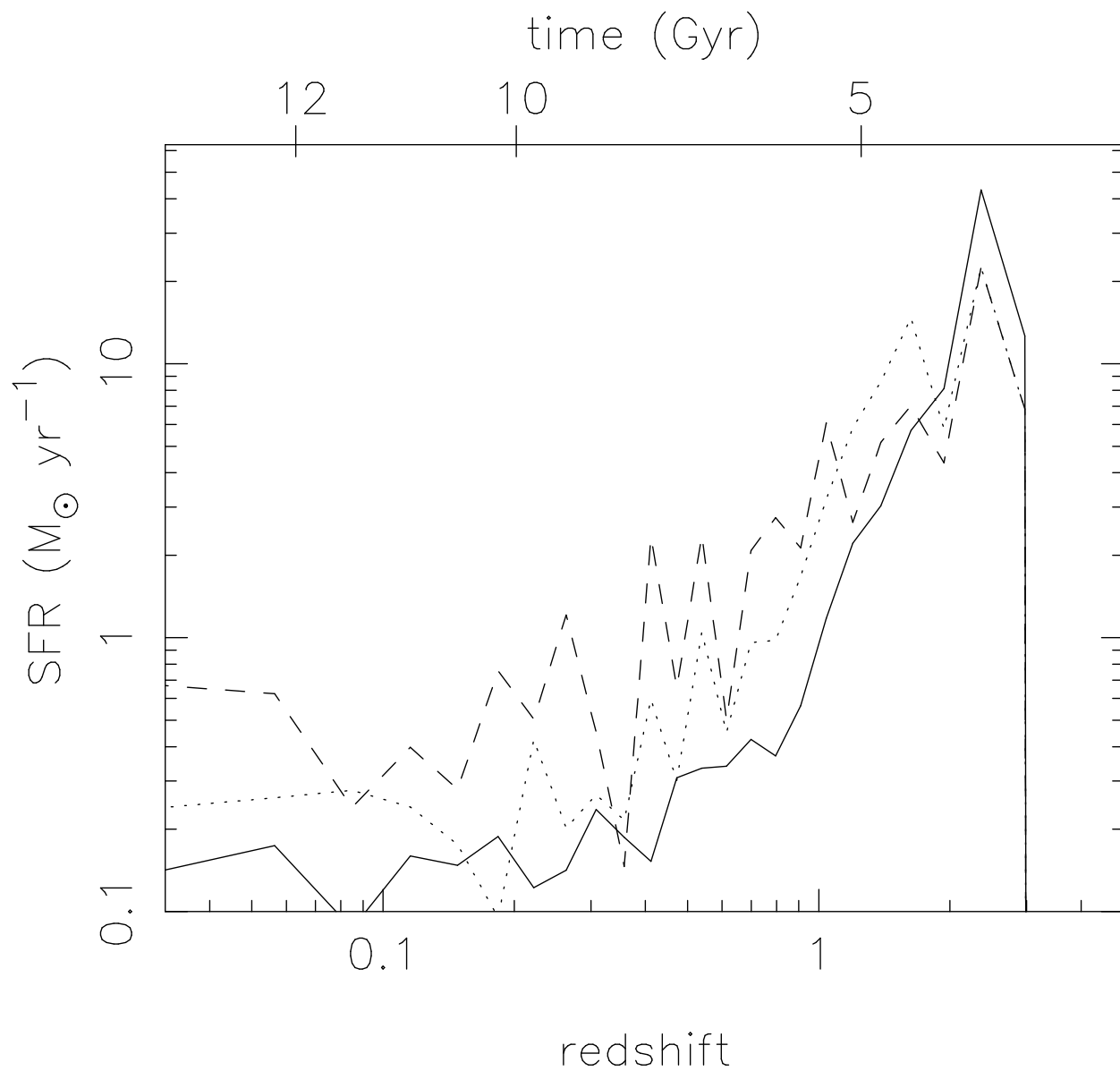


Fig. 5.— Evolution of the global star formation rate (SFR) of model 1 (solid line), model 2 (dashed) and model 3 (dotted).

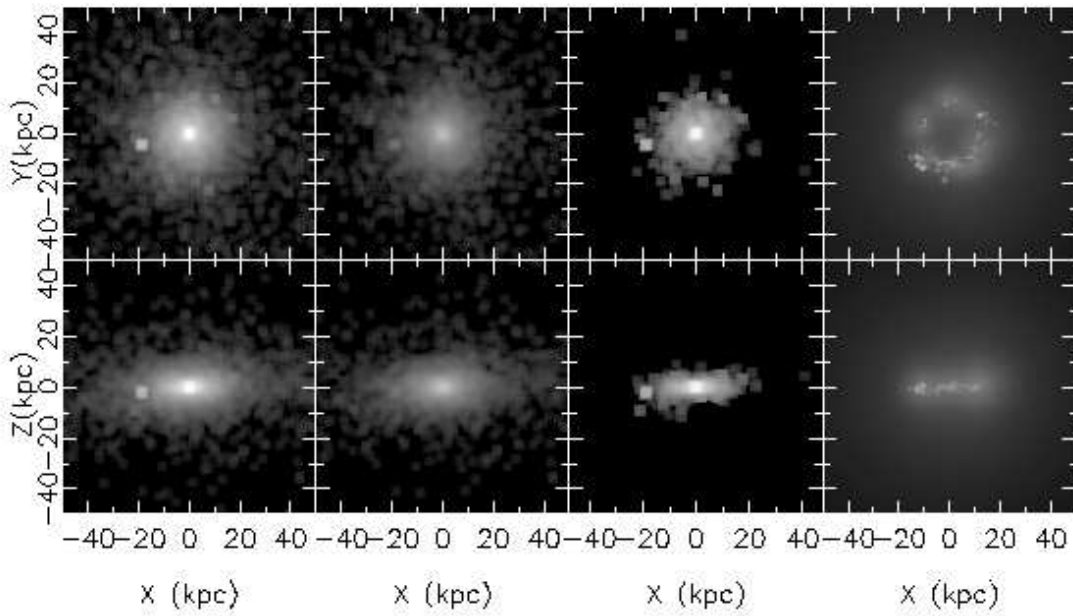


Fig. 6.— Density map of the final ($z = 0$) distribution of star particles (left panel), low-metallicity ($Z < 0.05Z_{\odot}$) stars, high-metallicity ($Z > 0.05Z_{\odot}$) stars, and gas particles, for model 3, in the X-Y (upper row) and X-Z (bottom row) planes.

white dwarfs by a similar amount to model 2, makes it an important component of chemodynamical models aimed at maximising the number of halo white dwarfs, while allowing higher metallicity stars to be distributed according to the Salpeter IMF.

We are further able to examine the ratio of white dwarf stars to main sequence stars in the halos of the three models. Using appropriate IMFs, we calculate $\sum_i^{halo} n_{WD,i}/n_{ms,i}$ giving a number ratio of white dwarf to main sequence stars in the halo region of 0.19 for model 1, 1.2 for model 2 and 1.0 for model 3. Here the number of white dwarfs is $n_{WD,i} = \int_{1M_{\odot}}^{8M_{\odot}} \Phi(m)dm$ if $t_{age,i} > 1$ Gyr and the number of main sequence stars is $n_{ms,i} = \int_{0.3M_{\odot}}^{1M_{\odot}} \Phi(m)dm$. We see that model 3 significantly increases the number of white dwarf halo stars, as required by our white dwarf halo scenario. This highlights that models 2 and 3 have resulted in creating a stellar halo which has a significant mass in the form of white dwarf stars. We found that this result was robust over a range of “regions” which could be used to define the halo. Unlike the values of densities quoted in Table 4, *this allows a comparison which is not directly sensitive to the region chosen as defining the halo.*

The differences in evolution and final morphology of models 1 and 2 from model 3 are not significant enough to show as separate diagrams in § 3, yet they do have some impact on the total stellar densities of our simulated halo region. Factors which will influence these differences are; the different ejected mass due to different IMFs result in different masses, and hence dynamics, of the remnant stellar particles; different ejecta also results in different gas enrichment and mass and different star formation rates (Figure 5); different cooling rates due to differences in metallicity of enriched gas particles; different energy feedback due to different supernova rates (although our implementation of such feedback is known to be highly inefficient in Tree-SPH codes). These are “secondary” effects of a different IMF on the white dwarf densities quoted in this section. As it is difficult to disentangle these effects, Table 4 shows the total halo stellar densities of the three models in order to indicate the magnitude of their combined effects. Here, total stellar density means the value of the summation of the mass of star particles in the halo region, divided by the volume of the halo region. There is little difference between the models in such total stellar densities and thus these secondary effects are not what drives the differences in white dwarf densities between the models. The difference in the number densities of white dwarfs between models can therefore be attributed to the variation of the adopted IMFs.

3.2. Chemical Constraints

In this section, we examine the constraints set by the observations of chemicals, in particular carbon, nitrogen and oxygen, set on the viability of our three models. We are

especially interested in whether the variable IMF of model 3 alleviates the problem of carbon and nitrogen overproduction relative to oxygen, as originally pointed out by GM97. Figure 7 shows the [C/O] and [N/O] abundance ratios as a function of global metallicity [Z]⁵ for the stellar particles in the solar neighbourhood for all models, to compare with observations of solar neighbourhood stars. We define the solar neighbourhood as the region bounded by $4 < R_{XY} < 10$ kpc and $|Z| < 1.5$ kpc. Carbon and nitrogen are highlighted due to the fact that their dominant nucleosynthesis sites are the intermediate mass white dwarf precursors under discussion here.

We constrain our models with the observed abundance distribution pattern of carbon, nitrogen, and oxygen seen in the metal poor Population II stars, which are dominated by halo stars (hashed regions in each panel of Figure 7). We remind the reader that Type Ia supernovae have not been included in the present analysis. As such, we take the total metallicity [Z] to act as a proxy for [Fe/H], without violating the validity of the simulations (since Type Ia supernovae are not critical contributors to the Galaxy’s CNO abundances). The points in Figure 7 correspond to those simulated star particles which reside, at the present-day, in the solar neighbourhood defined above - no kinematical (i.e., disk versus halo kinematics) cut was applied as the observational data we compare to, is of solar neighbourhood stars without kinematic selection.

The solid lines in each panel of Figure 7 correspond to the mass-weighted mean stellar metallicity of the simulation. For model 1, we can see that there is essentially no variation in [C,N/O] for halo metallicities (i.e., $[Z] < -1$), with the simulated halo particles occupying the same parameter space as the data (hashed regions). As the chemical enrichment from low- and intermediate- mass stars begins to become important, [C,N/O] approaches the solar ratio and the dispersion increases, both being in keeping with the observations of the solar neighbourhood distributions (Timmes et al. 1995). Not surprisingly, this is consistent with the conventional picture in which the sIMF (model 1) scenario is assumed to hold.

⁵[Z]= $\log_{10}(Z/Z_{\odot})$

Table 4: Total stellar and white dwarf number densities (in units of pc^{-3}) for the three models described here.

	model 1	model 2	model 3
Halo total stellar density	1.4×10^{-4}	1.5×10^{-4}	1.5×10^{-4}
Halo white dwarf density	1.7×10^{-5}	6.0×10^{-5}	6.5×10^{-5}

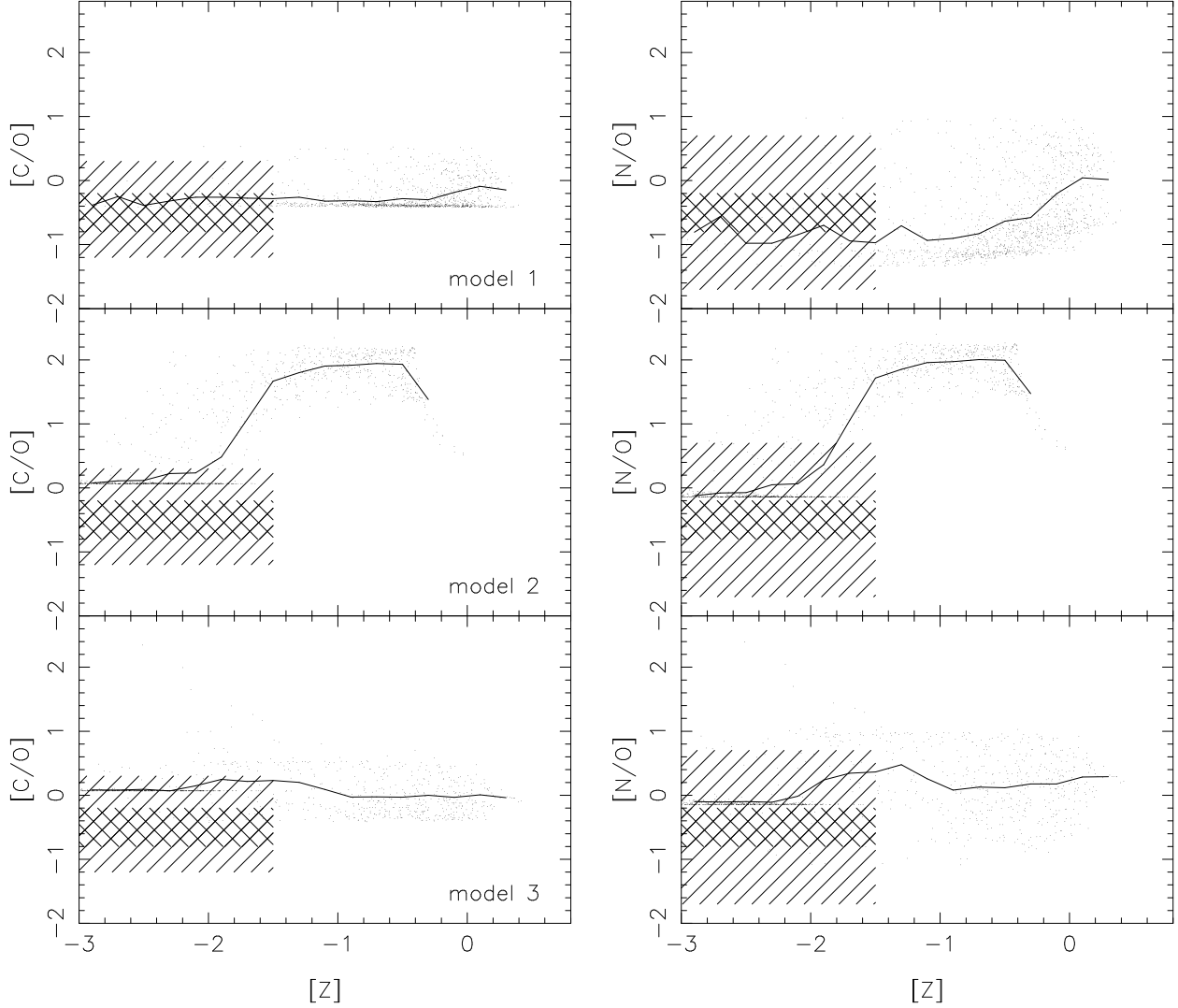


Fig. 7.— The values of $[C,N/O]$ for simulated star particles in the solar neighbourhood plotted against their metallicity $[Z]$ at redshift $z=0$. The results of model 1 are in the upper panels, below which are the results for models 2 and 3, respectively. The trend lines show the mass-weighted mean values of the simulations. The hatched regions correspond to the observational constraints listed by Timmes et al. (1995). All of the ~ 150 halo stars shown in Figures 13 and 14 of Timmes et al. lie within the bounds of the outer hatched regions, while $\sim 80\%$ of the sample lies within the inner regions.

Model 2 (middle panels of Figure 7) shows the clear signature of carbon and nitrogen overproduction. As the intermediate mass stars responsible for the nucleosynthesis of (the bulk of) these elements pass through the asymptotic giant branch, the resulting $[C/O]$ and $[N/O]$ quickly exceeds the halo observational constraints by more than two orders of magnitude - an invariant wdIMF model cannot be made consistent with the data (this is consistent with the analytical chemical evolution analysis of GM97).

The lower panels of Figure 7 demonstrate that model 3 (the variable IMF) does mitigate (somewhat) the overproduction of carbon and nitrogen at low metallicities. Below $[Z] \approx -1$, model 3 traces model 2; above $[Z] \approx -1$, the Salpeter (1955) component of the variable IMF begins to dominate star formation (and its associated element production), suppressing the extreme overproduction inherent in the invariant wdIMF model 2. Ultimately, $[C/O]$ and $[N/O]$ approach that of the model 1 (sIMF), reaching the scaled-solar ratio at $[Z] \sim 0$. While a definite improvement (in the sense that the factor of >100 overproduction in carbon and nitrogen seen in model 2 no longer exists), model 3 still leads to a factor of ~ 5 -10 carbon and nitrogen excess (with respect to oxygen) at metallicities in the range $-2.5 < [Z] < -1$.

A couple of features of the plots in Figure 7 are worth further comment here. In models 2 and 3 we notice a number of stars in a horizontal line with values of $[C,N/O] \sim 0$. These stars were formed from gas polluted by massive stars, prior to intermediate star's yields being ejected. Reference Table 1 which shows that the wdIMF massive star's ($> 10M_{\odot}$) integrated yields have $[C,N/O] \sim$ solar. Also note the limit of $[C,N/O]$ of ~ 2.2 in all models in Figure 7 which comes from the low metallicity intermediate mass stellar yields, as seen in Table 2.

4. Discussion

Ascribing the detection of the 13-17 microlensing events seen toward the LMC to an intervening halo white dwarf (WD) population implies that perhaps 20%–30% of Galaxy's dark matter is tied up in these stellar remnants (Alcock et al. 2000). This would correspond to a local WD halo number density of $\sim 2 \times 10^{-3} \text{ pc}^{-3}$. In contrast, Gould et al. (1998) concluded, using subdwarf star counts and an assumed Salpeter (1955) IMF, that the local spheroid WD number density was $2.2 \times 10^{-5} \text{ pc}^{-3}$ (i.e., two orders of magnitude smaller). More recently, the high proper motion survey for cool white dwarfs conducted by Oppenheimer et al. (2001) claimed a local halo WD number density of $2.2 \times 10^{-4} \text{ pc}^{-3}$.⁶ Whether

⁶The re-analysis conducted by Gibson & Flynn (2001) suggest that the Oppenheimer et al. (2001) number density should be revised downward by 40% to $1.3 \times 10^{-4} \text{ pc}^{-3}$.

the Oppenheimer et al. WDs are actually members of the halo, as opposed to the thick disk, is still a matter of debate (e.g. Gyuk & Gates 1999; Reid & Sahu 2001), although Hansen (2001) argues that if the halo is dominated by WDs, $\sim 80\%$ of these remnants lie beyond the detection limit of Oppenheimer et al. - i.e., the WD-dominated halo issue has not yet been resolved and future (deeper) surveys must be undertaken before the final word on the subject can be made.

Regardless of the current observational constraints, it is recognised that populating the Galactic halo with a dynamically-dominant WD component demands a significant modification to the underlying stellar IMF (e.g. GM97). A Chabrier (1996)-style IMF, peaked in the WD progenitor range, is one such possibility, although this IMF cannot apply at all times since we observe today a fairly conventional Salpeter (1955) or Scalo (1986)-like distribution. Metallicity may be the controlling factor in “switching” from the Chabrier-like to Salpeter-like IMF; a physical motivation for such a switch can be found in the studies of Yoshii & Saio (1987), Nakamura & Umemura (2001), Bromm et al. (2001) and Abel, Bryan & Norman (1999, 2001). Making our IMF dependent upon metallicity in our variable model is further motivated by the different MDF’s of the Galactic disk and halo regions; if one wishes to populate only the halo with large numbers of white dwarf stars, then it is the low metallicity stars which should have an IMF biased toward white dwarf progenitor stars. This appears necessary in order to explain MACHO observations by invoking white dwarf stars.

Our chemodynamical simulations employing a hybrid IMF (WD-dominated at metallicities $[Z] < -1.3$, and “conventional” at metallicities $[Z] > -1.3$) are successful in increasing the Galactic halo WD fraction (in comparison with models employing a Salpeter 1955 IMF alone) without violating present-day observable local carbon and nitrogen Pop II abundance constraints. These results are caused by low metallicity stars preferentially being found in the halo region as seen in Figure 6. Low metallicity stars are formed before and during the major star formation epoch caused by the collapse of the whole system. These stars are scattered by violent relaxation. Later, gas polluted by past star formation accretes smoothly and the metal rich disk component develops. This picture is consistent with previous chemodynamical studies of a Milky Way like galaxy (Steinmetz & Muller 1995; White et al. 2000; Bekki & Chiba 2001; Abadi et al. 2003). This metallicity segregation is what allows our simple variable IMF to populate the low metallicity stars of the halo with a large number of white dwarf stars. The discrepancy between observed metallicity distributions of Galactic halo and disk stars mean that our scheme of varying the IMF according to metallicity would seem appropriate, indeed necessary, if we are to explain MACHO events by white dwarfs.

That said, our best models were only capable of increasing the number of halo white dwarfs by a factor of 3-4 (Table 4) before violating the constraints of an overproduction of

carbon and nitrogen compared to oxygen. This factor is between our simulated models, and unlike the absolute densities is not significantly affected by the region selected as defining the halo. How does this factor relate to observed white dwarf densities? The Gould et al. value of $2.2 \times 10^{-5} \text{ pc}^{-3}$ assumes a Salpeter IMF; increasing this by a factor of 3-4 corresponds to halo WD mass fractions in of $\sim 1\text{-}2\%$ - halo WD mass fractions beyond this are not supported by our simulations.

Attempts to increase the halo WD fraction further necessitate significant revision to our fairly conventional star formation formalism. We attempted to force the halo WD issue by increasing substantially the efficiency of star formation (c_* in equation 1) in low-metallicity star-forming regions. We also tried decreasing the density threshold for star formation ρ_{crit} in these same regions.⁷ Both *ad hoc* revisions introduced moderate increases in the halo WD fraction. For example, increasing c_* by a factor of ten and decreasing ρ_{crit} by the same factor of ten, led to a halo WD density of $1.3 \times 10^{-4} \text{ pc}^{-3}$ (c.f. model 3 entries of Table 4). While such a density would be consistent a factor of ~ 8 increase of halo white dwarf densities over the Salpeter IMF model, this “extreme” model suffers from the same carbon and nitrogen overproduction which plagued model 2 (Section 3), mitigating its usefulness.

The hybrid IMF preferred here varies in a very simple manner and that the $0.05 Z_\odot$ transition metallicity for changing from the wdIMF to sIMF regime was a somewhat arbitrary choice. We found that adopting a lower metallicity for the transition (e.g. $0.01 Z_\odot$) does diminish the carbon and nitrogen overproduction, but at the expense of reducing the halo WD mass fraction. Thus, it becomes clear that a trade off exists between increased white dwarf halo densities and the overproduction of carbon and nitrogen compared to oxygen; any significant increases in white dwarf numbers are accompanied by worsening of the overproduction of carbon and nitrogen, as well as contamination of the disk with an unacceptable number of white dwarf stars. Our simulations suggest that attempts at increasing the number of halo white dwarf beyond that obtained in model 2 ($\sim 1\text{-}2\%$ of the halo, by mass) will violate these constraints.

Our best hybrid IMF model, while an improvement over purely WD-dominated IMF models, still overproduces stars with supersolar [C/O] and [N/O] ratios in the metallicity range $-2.5 < [Z] < -1$. Modifications to the star formation efficiency and threshold were incapable of eliminating this overproduction. As such, more extreme scenarios may need to be invoked in order to suppress the formation of these stars. An early Galactic wind, fine-tuned such that the carbon and nitrogen ejecta from the wdIMF component of our hybrid IMF is removed from the system before being incorporated into the stars which

⁷both these simulations were done using $n_{tot} = 18342$

ultimately form the Population II halo of the Milky Way, is one such potential modification (e.g. Fields et al. 1997; GM97). Although we do take into account the energy feedback of SNe (Section 2.1.3), our favoured model 3 does not develop a Galactic wind. That said, the exact efficiency of SNe feedback is uncertain; in a future work, we will explore more extreme feedback scenarios, in an attempt to suppress excess carbon and nitrogen overproduction at early times. At that time, we will also include the effects of Type Ia SNe, although we remind the reader that this inclusion has little impact upon the results shown here (as SNe Ia are negligible contributors to the carbon, nitrogen, and oxygen yields discussed here - see Section 2.1.3).

5. Summary

We have undertaken Galactic chemodynamical simulations of the formation and evolution of the Milky Way, exploring a region of parameter space designed to test the hypothesis that the Galaxy’s halo has a significant dynamical white dwarf component (perhaps as high as 30% by mass). This is the first numerical examination of the WD-dominated hypothesis, and a natural extension to the earlier semi-analytical investigation of Gibson & Mould (1997). Consistent with Gibson & Mould, we have found that carbon and nitrogen overproduction (by factors in excess of 100) are endemic to purely WD-dominated IMF models. For the first time, we have shown that a hybrid WD-dominated/Salpeter style IMF with a transition metallicity between the two of $Z = 0.05 Z_{\odot}$ can lead to a Milky Way model which is marginally consistent with virtually all available present-day constraints. A mild overproduction of carbon and nitrogen remains (although this overproduction is reduced by more than an order of magnitude); an early Galactic wind may alleviate this overproduction, an hypothesis we will explore in a future study. Our best model can lead to a halo WD mass fraction a factor of ~ 4 greater than expected with a more conventional IMF (corresponding to $\sim 1 - 2\%$ of the mass of the halo), but values in excess of this cannot be accommodated within our chemodynamical framework.

Acknowledgments

We acknowledge the support of the Australian Research Council through its Large Research Grant Program (A0010517). CB acknowledges receipt of an Australian Postgraduate Award. We thank Chris Flynn for his helpful advice during the completion of this manuscript. The simulations described here were performed at the Victorian Partnership for Advanced Computing and the Beowulf Cluster at the Swinburne University Centre for

Astrophysics & Supercomputing.

REFERENCES

- Abia, C., Dominguez, I., Straniero, O., Limongi, M., Chieffi, A., Isern, J., 2001, *ApJ*, 557, 126
- Abel, T., Bryan, G., Norman, M., 1999, 2 in *Space*, meeting held in Paris, France, September 28th - October 1st, 1999. Eds.: F. Combes, G. Pineau des Forets. Cambridge University Press, *Astrophysic Series*
- Abel, T., Bryan, G., Norman, M., 2002, *Science*, Volume 295, Issue 5552, 93-98
- Adams, F.C., Laughlin, G., 1996, *ApJ*, 468, 586
- Alcock, C., et al., 2000, *ApJ*, 542, 281
- Barnes, J.E., Hut, P., 1986, *Nature*, 324, 446
- Beers, T.C., et al., 2002, *AJ*, 124, 931
- Bekki, K., Chiba, M., 2001, *ApJ*, 558, 666
- Bertschinger, E., 1995, *astro-ph/950607*
- Bromm, V., Ferrara, A., Coppi, P. S., Larson, R. B., 2001, *AAS*, 198, 603
- Chabrier, G., Segretain, L., Mera, D., 1996, *ApJ*, 486, L21
- Dominguez, I., Straniero, O., Limongi, M., Chieffi, A., 1999, *ApJ*, 524, 226
- Fields, B.D., Freese, K., Graff, D.S., 2000, *ApJ*, 534, 265
- Flynn, C., Gould, A., Bahcall, J., 1996, *ApJ*, 466, L55
- Flynn, C., Holopainen, J., Holmberg, J., 2002, *MNRAS*, submitted (*astro-ph/0202244*)
- Flynn, C., Sommer-Larsen, J., Fuchs, B., Graff, D.S., Salim, S., 2001, *MNRAS*, 322, 553
- Freeman, K., Bland-Hawthorn, J., 2002 *ARAA*, 40, 487
- Gibson, B.K., Flynn C., *Science*, 292, 2211
- Gibson, B.K., Mould, J.R., 1997, *ApJ*, 482, 98 (GM97)

- Gilmore, G., 2001, in Tacconi, L.J., Lutz, D., eds, *Starbursts: Near and Far*, Springer-Verlag, Heidelberg, p. 34
- Gingold, R.A., Monaghan, J.J., 1977, *MNRAS*, 181, 375
- Goldman, B., Afonso, C., Alard, Ch., et al., 2002, *A&A*, in press (astro-ph/0205537)
- Gould, A., Flynn, C., Bahcall, J., 1998, *ApJ*, 503, 798
- Gyuk, G., Gates, E., 1999, *MNRAS*, 304, 281
- Hansen, B.M.S., *Nature*, 1998, 394, 798
- Hansen, B.M.S., 2001, *ApJ*, 558, L39
- Harris, H.C., et al., *ApJ*, 2001, 549, L109
- Hernquist, L., Katz, N., 1989, *ApJS*, 70, 419
- Hodgkin, S.T., et al., *Nature*, 2000, 403, 57
- Ibata, R.A., Richer, H.B., Gilliland, R.L., Scott, D., 1999, *ApJ*, 524, 95
- Ibata, R.A., Irwin, M., Bienaymé, O., Scholz, R., Guibert, J., 2000, *ApJ*, 532, L41
- Käelländer, D., Hultman, J., 1998, *A&A*, 333, 399
- Katz, N., 1992, *ApJ*, 391, 502
- Katz, N., Gunn, J.E., 1991, *ApJ*, 377, 365
- Katz, N., Weinberg, D.H., Hernquist, L., 1996, *ApJS*, 105, 19
- Kay, S.T., Pearce, F.R., Jenkins, A., et al. 2000, *MNRAS*, 316, 374
- Kawata, D., 1999, *PASJ*, 51, 931
- Kawata, D., 2001, *ApJ*, 548, 703
- Kawata, D., Gibson, B.K. 2003, in preparation
- Kobayashi, C., Tsujimoto, T., Nomoto, K., Hachisu, I., Kato, M., 1998, *ApJ*, 503, 155
- Kotenova, E., Flynn, C., Chiappini, C. & Matteucci, F. 2002, *MNRAS*, 336, 879
- Koopmans, L.V.E., Blandford, R.D., 2002, *MNRAS*, submitted (astro-ph/0107358)

- Kroupa, P. 2001, MNRAS, 322, 231
- Lasserre, T., et al., 2000, A&A, 355, 39
- Leggett, S.K., Ruiz, M.T., Bergeron, P., 1998, ApJ, 497, 294
- Lucy, L., 1977, AJ, 82, 1013
- Marigo P., Bressan, A., Chiosi, C., 1996, A&A, 313, 545
- Marigo, P., Girardi, L., Chiosi, C., Wood, P.R. 2001, A&A, 371, 152
- Mendez, R.A., 2002, A&A, in press (astro-ph/0207569)
- Mendez, R.A., Minniti, D., 2000, ApJ, 529, 911
- Mera, D., Chabrier, G., Schaeffer, R., 1998, A&A. 330, 953
- Morrison, H. L. 1993, Astron. J., 106, 578
- Nakamura, F., Umemura, M., 2001, ApJ, 548, 19
- Nelson, C.A., Cook, K.H., Axelrod, T.S., Mould, J.R., Alcock, C., 2002, ApJ, in press (astro-ph/0112414)
- Oppenheimer, B.R., et al. 2001, Science, 292, 698
- Reid, N., Sahu, K.C., Hawley, S., 2001, ApJ, 559, 942
- Renzini, A., Voli, M., 1981, A&A, 94, 175
- Reylé, C., Robin, A.C., Crézé, M., 2001, A&A, 378, L53
- Ryan, S.G. & Norris, J.E., 1991, AJ, 101, 1865
- Richer, H.B., 2001, in Livio, M. ed, The Dark Universe: Matter, Energy and Gravity, Cambridge Univ. Press, Cambridge, in press (astro-ph/0107079)
- Salpeter, E.E., 1955, ApJ, 121, 161
- Sauman, D., Jacobson, S.B., 1999, ApJ, 511, L107
- Scalo, J.M., 1986, Fund. Cosm. Phys., 11, 1
- Schaller, G., Schaerer, D., Meynet, G., 1992, A&AS, 96, 269
- Steinmetz, M., Muller, E., 1995, MNRAS, 276, 549

- Sutherland, R.S., Dopita, M.A., 1993, ApJS, 88, 253
- Theis, C., Burkert, A., Hensler, G., 1992, A&A, 265, 465
- Timmes, F.X., Woosley, S.E., Weaver, T.A., 1995, ApJS, 98,617
- Torres, S., García-Berro, E., Burkert, A., Isern, J., 2002, MNRAS, in press (astro-ph/0207113)
- van den Hoek L.B., Groenewegen M.A.T., 1997, A&AS, 123, 305
- White, S.D.M., Springel V., 2000, in A. Weiss, T.G. Abel, V. Hill, eds, The First Stars, Spinger-Verlag, Heidelberg, p. 327
- Wilkinson, M.I., Evans, N.W., 1999, MNRAS, 310, 645
- Woosley S.E., Weaver, T.A., 1995, ApJS, 101, 181
- Yoshii, Y., Saio H., 1986, ApJ, 301, 587
- Zaritsky, D. in B.K. Gibson, T.S. Axelrod, M.E. Putman, eds, The Third Stromlo Symposium: The Galactic Halo ASP Conference Series, Vol 165, 1999, p. 34